Two methods on one stone: integrating visual and analytical techniques to clarify lithic raw material utilization in the Middle and Later Stone Age at Umhlatuzana rockshelter (South Africa)

Sifogeorgakis, E.; Schmid, V.; Van Os, B.; Fratta, V.; Huisman, H.; Dusseldorp, G.L.

Journal of Archaeological Science: Reports 48 (2023) 103890

Contents lists available at ScienceDirect

Journal of Archaeological Science: Reports

journal homepage: www.elsevier.com/locate/jasrep

Two methods on one stone: Integrating visual and analytical techniques to clarify lithic raw material utilization in the Middle and Later Stone Age at Umhlatuzana rockshelter (South Africa)

Irini Sifogeorgaki [a,*], Viola C. Schmid [a,b,c], Bertil van Os [d], Vi Fratta [a], Hans Huisman [d,e], Gerrit L. Dusseldorp [a,f]

[a] Human Origins, Faculty of Archaeology, Leiden University, Leiden, Netherlands
[b] Department of Early Prehistory and Quaternary Ecology, Eberhard Karls Universität Tübingen, Tübingen, Germany
[c] UMR 7041, Equipe AnTET, Université Paris Ouest Nanterre La Défense, Nanterre Cedex, France
[d] Section Archaeology, Cultural Heritage Agency of the Netherlands, Amersfoort, Netherlands
[e] Groningen Institute for Archaeology, University of Groningen, Groningen, Netherlands
[f] Palaeo-Research Institute, University of Johannesburg, Johannesburg, South Africa

ARTICLE INFO

Keywords:
Raw material identification
Micromorphology
p-XRF
Lithics
Stone Age
South Africa

ABSTRACT

We develop a study protocol to efficiently and accurately identify the raw material categories constituting the lithic assemblages at Umhlatuzana rockshelter, South Africa. We combine visual and analytical methods to establish a raw material database and to provide a more accurate insight into raw material selection during the Pleistocene Middle and Later Stone Age occupational sequence of Umhlatuzana. The protocol combines petrological properties (as studied on micromorphological samples), elemental composition of the specimens (as measured with p-XRF) and visual characterization by lithic analysts. We tested the protocol by applying it to a sample of piece-plotted lithics from four spits across the stratigraphic sequence. We document the intensive use of sandstone accounting for 25% of the tested sample. We also report a larger importance of hornfels and lower proportion of quartz than was reported in previous analyses (Kaplan 1990). The combination of micromorphological and p-XRF analysis of the Umhlatuzana assemblages demonstrates that with only visual inspection, the variability of raw materials used may be misinterpreted. With accurate raw material datasets, we are better equipped to answer techno-economic questions of the southern African Stone Age.

1. Introduction

Due to its durable nature, stone is the best-represented cultural material in the archaeological record. The properties of different types of rocks (i.e., availability, ease of extraction, knapping qualities, and durability/sharpness of working edges) interact with the functional demands of toolkits to shape prehistoric raw material preferences (e.g., Porraz et al., 2016; Soressi and Geneste, 2011). Secure raw material identification is a necessary first step in the study of raw material selection and use in the past, consequently allowing to make inferences on land use patterns and group mobility. The archaeological record shows that isotropic amorphous material such as obsidian glass, chert and flint was the material of choice for lithic tool production as these propagate conchoidal fracture well. Especially in regions where such materials were not available, raw material with less optimal properties such as quartzites, hornfels or dolerite were used. Since the archaeological toolbox for lithic artefact determination is primarily based on amorphous material having similar properties and showing similar technical features (e.g., Archer et al., 2018; Bertouille, 1989; Bordes, 1947; Pelegrin, 2000; Dibble and Rezek, 2009), research into the expression of knapping stigmata of other rock types is less prominent (e.g., Cologne and Mourre, 2009; Kieffer and Raynal, 2007; Mourre, 1996).

To further comprehend raw material preference, acquisition, and provisioning strategies, more secure identification protocols are needed. We examine one such instance in the Late Pleistocene of South Africa and develop a procedure that results in an improved understanding of raw material representation throughout the past 70,000 years of Umhlatuzana rockshelter (hereafter UMH). Archaeological raw material

* Corresponding author at: Leiden University, Faculty of Archaeology, Van Steenis, Einsteinweg 2, 2333 CC Leiden, Office A1.16, Netherlands.
E-mail address: e.sifogeorgakis@arch.leidenuniv.nl (I. Sifogeorgaki).

https://doi.org/10.1016/j.jasrep.2023.103890
Received 8 May 2022; Received in revised form 9 February 2023; Accepted 10 February 2023

classification is usually done on macroscopic grounds, as would material selection in the past together probably with haptic evaluations (e.g., Andrefsky and Andrefsky, 1998; Saini-Eidukat and Michlovic, 2005; Will, 2021). Nevertheless, petrographic and geochemical analyses (i.e., microscopic mineral and stone identification combined with chemical analyses and crystallography) allow for enhanced stone type determinations that can aid in determining the raw material sources that were exploited (e.g., Brandl et al., 2018; Delvigne et al., 2019; Favreau et al., 2020; Prieto et al., 2020; Sánchez de la Torre et al., 2020; Šarić et al., 2021; Skarpelis et al., 2017; Wadley and Kempson, 2011). A macroscopic raw material identification approach was also used for the lithic analysis of UMH from the 1980 s excavations (Kaplan, 1989; 1990).

UMH is an important archaeological site for the study of the Middle Stone Age (MSA) and Pleistocene Later Stone Age (LSA) in South Africa with a largely continuous occupation sequence spanning MIS 4–2 (~70,000–10,000 BP) (Kaplan, 1990; Lombard et al., 2010). Changing raw material selection is a crucial aspect of the Middle to Later Stone Age transition that appears characterized by a shift in stone raw material use, reduction strategies, typological corpus, and continuities or discontinuities in provisioning strategies in addition to the technological organization (e.g., Barut, 1994; Clark, 1997; Grove and Blinkhorn, 2020; Mackay et al., 2014; McCall and Thomas, 2009; Pargeter, 2016; Porraz et al., 2016; Shipton et al., 2018; Steele et al., 2016; Tryon and Faith, 2016). The current study was prompted by a mismatch in raw material ratios between the old (Kaplan, 1989; 1990) and renewed (Sifogeorgaki et al., 2020) excavations. Since UMH is one of the few sites bearing MSA-LSA transitional assemblages in southern Africa, a possible raw material misidentification leads to erroneous input for overview papers and statistical *meta*-analyses (e.g., McCall and Thomas, 2009).

UMH was first excavated in 1985 by Jonathan Kaplan. His macroscopic analysis of the lithic assemblages from the Pleistocene deposits suggests that quartz was most abundant (61 %) followed by hornfels (38 %) with a minor presence of quartzite (1 %) (Kaplan, 1990). In 2018 and 2019, renewed excavations were conducted by a team from Leiden University (Reidsma et al., 2021; Sifogeorgaki et al., 2020). The research was mainly geoarchaeological in character: overall 0,75 m^2 were excavated and samples were acquired for an abundance of analyses (e.g., micromorpholgy, OSL, phytoliths, etc; see Sifogeorgaki et al., 2020). This small excavation yielded very large archaeological assemblages with 8170 piece-plotted lithic finds. Rather unexpectedly, preliminary raw material determinations of the lithic finds and micromorphology samples were at odds with the results reported in previous analyses. Our initial lithic analysis did not yield a small group of quartzite artefacts as we expected but larger quantities of quartzite or sandstone pieces. This prompted the development of a raw material identification protocol to verify the representation of the different lithologies in the artefact assemblages that we report on here.

To achieve this, we initiated a multi-layered petrological and elemental classification of the lithic artefacts. Initially, we distinguished six raw material categories based on micr omorphological thin section analysis: sandstone, hornfels, quartz, dolerite, siltstone, and silcrete. We then determined the elemental composition of the raw materials from the micromorphology samples using p-XRF and also conducted p-XRF analysis on single lithic artefacts. This allowed us to determine the elemental characteristics of the raw materials used and to investigate raw material distribution in different deposits across the chrono-cultural sequence. Additional raw material categories (ironstone) and variations within existing categories (e.g., heavy mineral sandstone) were identified after the p-XRF analyses.

2. Background

2.1. Umhlatuzana rockshelter geological and geomorphological setting

UMH is located approximately 35 km west of Durban in the Province KwaZulu-Natal, South Africa (Fig. 1A). The site is situated along a steep cliff at the edge of the Umhlatuzana River valley, approximately 60 m above the riverbed. The rockshelter faces northeast and is 47 m long, 8 m wide, and circa 17.5 m high (Fig. 1B). Geologically, the area is characterised by medium to very coarse-grained feldspar sandstones and fine-grained quartz arenites belonging to the Ordovician Natal Group Formation. UMH is situated within a quartz arenite sandstone bedrock which is at places interspersed with thin shale layers (Reidsma et al., 2021). Outcrops belonging to the Namaqua-Natal metamorphic province are documented within close proximity to the rockshelter (Fig. 2). Those consist of coarse-grained biotite granite (Oribi Gorge Suite) as well as gneiss, amphibolite, and other regional metamorphic rocks (Mapumulo Group) (Durban 1:250.000 geological map). As a result of contact metamorphism, hornfels and quartzite are expected to be formed around the Oribi Gorge Suite granite. It is important to note that some older sandstone classifications used in South Africa categorized sandstones (mainly quartz arenites) as quartzites (Adams, 1984; Howard, 2005).

2.2. Umhlatuzana rockshelter research history

The site of UMH was discovered in 1982 during the construction of the N3 Johannesburg-Durban highway (Kaplan,1990). A rescue excavation was undertaken by Jonathan Kaplan in 1985 who excavated squares K2, K3, J2, and J3 to bedrock (~2.65 m depth) and K1 and J2 to ~ 1.5 m depth (Kaplan, 1989; 1990; for excavation map see Reidsma et al., 2021, Fig. 3). Kaplan's excavation yielded over 1.25 million stone artefacts, most of which were categorized as waste (Kaplan, 1990: Table 3). McCall and Thomas (2009) made use of the data published by Kaplan (1990) in a statistical investigation of changes in lithic assemblage characteristics across the MSA-LSA transition. Several studies concerning specific aspects of the lithic materials from the MSA strata were published (Archer et al., 2016; Högberg and Lombard, 2016a, b; Lombard 2007; Lombard et al., 2010; Mohapi, 2008; 2013). Lombard et al. (2010) also initiated a small-scale fieldwork campaign to conduct optically stimulated luminescence (OSL) dating of the MSA deposits. In 2018 and 2019, a team from Leiden University in collaboration with the KwaZulu-Natal Museum conducted high-resolution excavations of UMH (Sifogeorgaki et al., 2020). Three sub- squares, namely L3a, L2b, and L2a were excavated to a depth of 2 to 2.4 m with the goal of clarifying the stratigraphy and chrono-cultural sequence of the site (Sifogeorgaki et al., 2020).

2.3. Umhlatuzana rockshelter stratigraphy and chrono-cultural sequence

The stratigraphy was divided into two principal groups: the lower Group P (Pleistocene) and the upper Group H (Holocene) (Sifogeorgaki et al., 2020). Group P deposits (Units P1 to P17) appear homogenous with a lack of clear stratigraphic boundaries. During excavation, the deposits were subdivided into units and to increase stratigraphic control during excavation, the units were excavated in ~ 2 cm horizontal spits (see Table 1 for correspondence of spits to units). Analysis of the find density allowed the grouping of the deposits into a series distinct higher (ZH1 to ZH4) and lower (ZL1 to ZL3) find-density zones (Reidsma et al., 2021; Sifogeorgaki et al. 2020). A pronounced lateral difference in sediment moisture content was also recognized (Sifogeorgaki et al., 2020). The application of OSL to the lowermost deposits of the sequence suggested a date of 70.5 +/- 4.7 ka for the deposits directly on top of the bedrock (Lombard et al., 2010, also see Sifogeorgaki et al., 2020). Group H deposits (Units H1 to *H*10) are characterized by well-defined stratigraphic boundaries with a clear presence of anthropogenic and biogenic features (Sifogeorgaki et al., 2020). The only geogenic sediment inputs affecting UMH derive from the rockshelter's bedrock through attrition and rockfall (Sifogeorgaki et al., 2020). As a result, except for sandstone, all of the raw material categories found at the rockshelter have an anthropogenic origin (Table 2).

Fig. 1. A. Map indicating the location of Umhlatuzana rockshelter and nearby sites. Map modified after Sifogeorgaki et al. (2020). B. West view of the site. Image by JD.

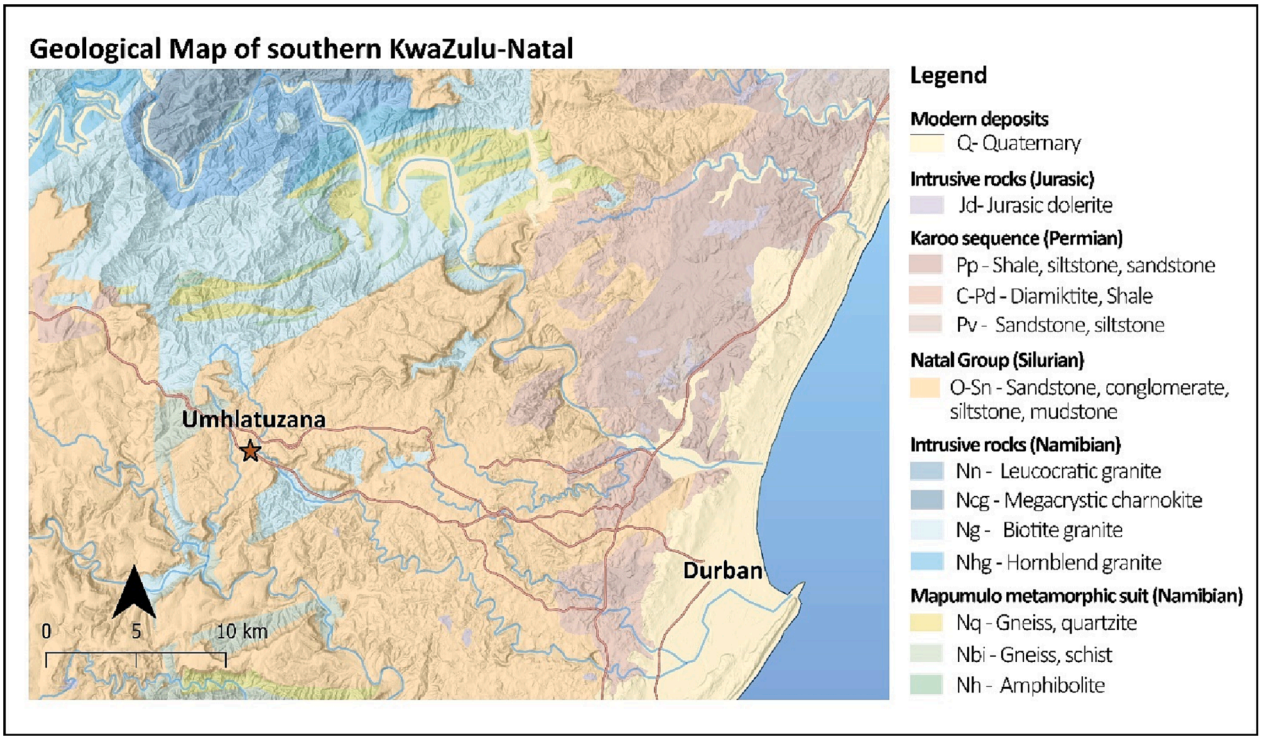

Fig. 2. Simplified geological map of the area surrounding Umhlatuzana rockshelter. Map is modified after the Durban 1:250.000 geological map (Department of Mineral and Energy Affairs, Sheet 2930) using QGIS 3.16.16.

Kaplan (1990) identified the following technocomplexes: pre-Howiesons Poort, Howiesons Poort, late MSA, MSA/LSA transition, and Robberg (LSA). Subsequent work by Lombard et al. (2010) established that the pre-Howiesons Poort contains Still Bay bifacial points. Our initial typological survey confirms the main elements that Kaplan identified (Sifogeorgaki et al. 2020), but more detailed lithic technological analyses are ongoing (Schmid et al. in prep).

3. Materials and methods

3.1. Sample selection

To understand the represented rock types, we first examined the lithic materials represented in micromorphological thin sections and soil blocks of the site. The determination of our main raw material lithologies is based on micromorphological analysis of 9 samples (total 15 thin sections) deriving from Group P deposits of square L3a (see also section 3.3.2) (Fig. 3). This square is associated with one of Kaplan's documented main excavation profiles, K3/L3 section (Kaplan, 1990: Fig. 8, p7). Subsequently we studied a sample of the excavated piece-

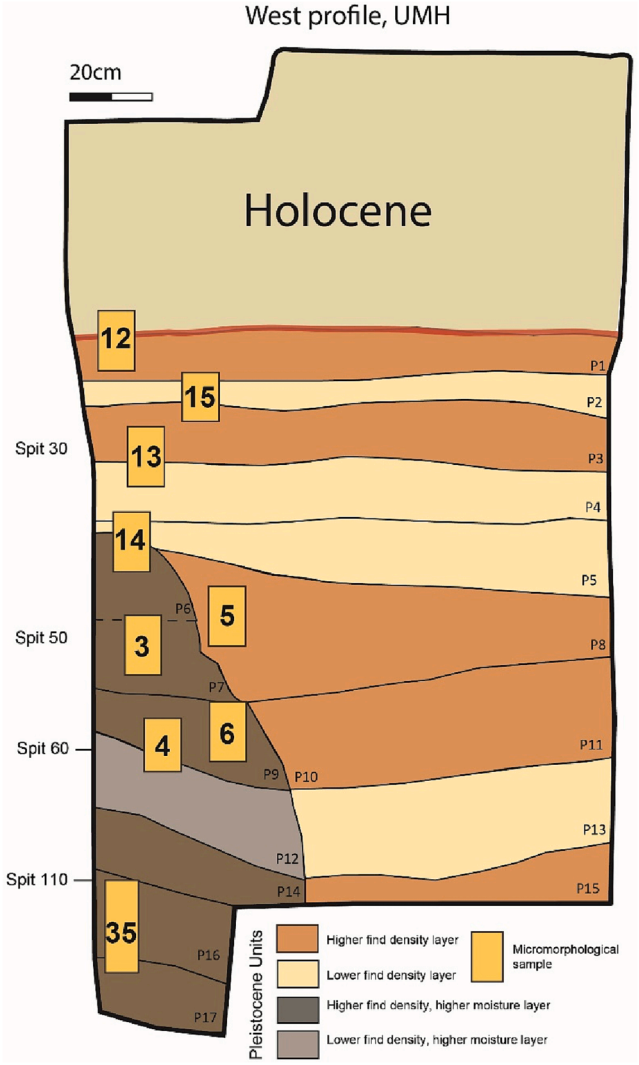

Fig. 3. Simplified stratigraphic drawing from the 2018–2019 excavations focusing on Group P deposits of the west profile at Umhlatuzana rockshelter. For the stratigraphic location of the analysed spits of piece-plotted materials, refer to Table 1. The micromorphology sample locations, and spit heights (2018–2019 excavation) are indicated on the drawing.

plotted finds. The analyzed finds (total count: 178) derive from L3a spits bearing LSA (Spit 30: 32 finds), transitional MSA/LSA (Spit 50: 74 finds) and MSA (Spit 60: 23 finds, Spit 110: 48 finds) industries (Fig. 3, Table 4). These spits were selected because they represent different cultural entities and because they are in close proximity to the micromorphology samples. This study focused on material defined as 'stone' during the excavation, including both natural pieces and artefacts in the case of sandstone. Rocks rich in iron oxides classified as 'ochre' are excluded from these analyses but will be the focus of future studies.

3.2. Study protocol

To link the rock types identified in the thin sections with the piece-plotted archaeological materials, we use their petrological properties and elemental composition as measured with p-XRF. We determined the raw material categories through petrological analysis using standard geological definitions. We also conducted a first elemental characterization using p-XRF on the micromorphology blocks associated with the analyzed thin sections. Next, we selected artefacts from excavated spits that are associated with the micromorphological samples (Fig. 3). We first assessed the artefact raw material categories macroscopically. We then used p-XRF to determine their elemental signal documenting the position where the measurement was taken. We re-examined (macroscopically and through supplementary p-XRF analysis) the cases in which the macroscopic and XRF raw material determinations were inconsistent. When a group of lithic artefacts yielded a discrete p-XRF elemental signal, we created a new descriptive raw material category.

3.3. Raw material analysis methods

3.3.1. Macroscopic analysis

The raw material categories of the cleaned artefacts were macroscopically identified (unaided eye and with the use of a 20x magnifying glass). The surface characteristics of the stone artefacts were also explored using a stereoscopic microscope.

3.3.2. Micromorphology

The initial characterization of the lithologies present at UMH is based on the petrographic analysis of stone fragments present in micromorphological thin sections. Intact sediment samples were taken from the west profile of the renewed excavations using plaster of Paris (Stoops and Nicosia, 2017). The samples were prepared at the laboratory of the Cultural Heritage Agency of the Netherlands (RCE) in Amersfoort using the preparation protocol from Reidsma and colleagues (2021). For this study, 15 petrographic thin sections of 30 μm thickness were analyzed primarily using a Euromex IS.1053-PLPOLi polarization microscope with 10x/23 mm eyepiece and trinocular, and magnifications from 5 to 40x. Their mineralogy was identified using petrographic literature and resources (e.g., Adams et al., 1984; Barker, 2014; MacKenzie and Adams, 1994). For the description of the micromorphology results we follow abundancy terminology by Stoops (2003): frequent 31–50 %; common 16–30 %; few 5–15 %; very few < 5 %.

3.3.3. Portable X-ray fluorescence analysis

The p-XRF measurements were conducted at the RCE using a Thermo Scientific Niton XL5 energy-dispersive hand-held XRF analyzer, equipped with a silicon drift detector with an in-built object camera to control sample position. A portable test stand was used for the analyses to assure stable measurement conditions. All artefacts and stones were cleaned by carefully removing adhering soil material and other debris. Care was taken to position the sample surfaces parallel to the XRF window. Two measurements were taken on the stones exposed on the micromorphology slabs in order to ensure that the measurements were of the stone sections and not of the surrounding matrix. One measurement was taken on the excavated lithics. Studies elsewhere show that multiple measurements generally replicate each other and so suggest one reading is sufficient (Theys et al., 2019). In view of this and since we wanted to differentiate between different rock types, we do not require very detailed elemental mapping of the specimens, one measurement suffices. Additional measurements were taken for outliers and in cases where the macroscopic and XRF raw material determination were not in agreement. The Cu/Zn-mining mode was selected, with a measuring time of 110 s using 4 sequential energy settings: Light range (Mg to Cl) at 8 kV 200 mA, low range (K to Ti) at 20 kV 100 mA, main range (V to Ag including L-lines for Pb) and high range (Cd- Ba) both at 50 kV, 40 mA (Huisman et al., 2017). The machine was calibrated using a set of 14 powdered ISE standard samples (www.wepal.nl). For more details on the analysis protocol and calibration see Huisman et al. (2017).

The quantification of light elements is semi-quantitative at best due to mineralogical effects, inhomogeneity and the absorption of the secondary X-rays, especially in the low kV range (0.5–4.0 kV). To overcome these effects, samples should have been ground and or fused with lithiumtetra/ metaborate to a glass bead (Potts and Webb, 1992), which was not possible with the archaeological artefacts. Instead of focusing on light element distribution, elements such as Rb and Sr can be used as a proxy for feldspar and clays while TiO_2 and Zr can be used as proxy for heavy minerals (Calvert and Pedersen, 2007), as the secondary X-rays of

Table 1
Raw material distribution and lithic industries within different layers at Umhlatuzana rockshelter based on the 1985 excavation (Kaplan, 1990). Spits and Units as per the 2018–2019 excavations (Sifogeorgaki et al, 2020). The cut off size of the excavated finds (column Total (N)) is not mentioned.

Spits (L3a)	Units	Kaplan excavation						Industry
		Context	Quartz (%)	Hornfels (%)	Quartzite (%)	Chert (%)	Total (N)	
15–16	H10, P1	Layer 5	79.7	15.1	3	2.2	16,829	Later Stone Age
17–21	P1	Layer 6	76.5	18.9	2.3	2.2	17,687	
22	P1, P2							
23–24	P2	Layer 7	72.6	23.4	3	1	18,264	
25–26	P3							
27–29	P3	Layer 8	71.4	24.6	3.1	0.9	21,599	
29–31	P3	Layer 9	77.6	19.4	2.5	0.5	21,926	
32	P3, P4							
33–34	P4	Layer 10	76.5	21.2	2.1	0.3	18,140	
35–39	P4	Layer 11	78	19.4	2.3	0.3	19,055	
40–42	P4, P6	Layer 12	76.7	21.7	1.4	0.2	22,419	
43	P6, P8	Layer 13	79.7	19	1.1	0.1	30,721	
44–46	P6, P8	Layer 14	70.2	28.7	0.9	0.1	52,464	MSA/LSA transition
47–48	P6	Layer 15	58.4	40.4	1.2	0.1	53,846	
48	P7							
47–48	P8							
49–51	P7, P8	Layer 16	32.6	66.2	1.2	0.1	42,763	
51–53	P7, P8	Layer 17	18.5	80.1	1.3	0	39,743	
54	P7, P8	Layer 18	15.9	82.6	1.6	0	67,052	
55–56	P9							
57–58	P9	Layer 19	11.3	87.4	1.3	0	70,408	Middle Stone Age
59–61	P9, P12	Layer 20	15.6	82.2	2.2	0	38,899	
62–63, 100	P12	Layer 21	34.5	61	4.5	0.1	17,019	
101–104	P12, P14	Layer 22	59.5	38.5	2	0	27,665	
105–109	P14, P16	Layer 23	77	21.9	1.1	0	87,592	
110–114	P16	Layer 24	81.2	18.6	0.2	0.1	110,043	
115–118	P16	Layer 25	82.2	16.9	0.8	0	88,601	
119–122	P17, P16	Layer 26	78.2	20.6	1.1	0	69,250	
123–125	P17	Layer 27	80.3	17.8	1.8	0	43,307	
		Layer 28	81.1	17.4	1.4	0.1	22,360	
		Total	**62.2**	**38.3**	**1.4**	**0.2**	**1,017,652**	

Table 2
Chemometric element conditions used to determine raw material categories based on p-XRF measurements from lithics deriving from Umhlatuzana rockshelter. The element conditions are site specific.

Raw Material	Element condition (p-XRF measurement)				
Quartz	Total - (SiO_2, Al_2O_3, P_2O_5) < 5	Zr < 20			
Sandstone	Total - (SiO_2, Al_2O_3, P_2O_5) < 8	Zr > 20	Rb < 100		
Hornfels	Total - (SiO_2, Al_2O_3, P_2O_5) > 8	Zr > 20	Rb > 100		
Hornfels ↓ K_2O ↑ CaO	Total - (SiO_2, Al_2O_3, P_2O_5) > 8	Zr > 20	Rb < 100	CaO > 2	Fe_2O_3 > 10
Chert	Total - (SiO_2, Al_2O_3, P_2O_5) > 8	Zr > 20	Rb < 100	Fe_2O_3 < 10	
Ironstone	Fe_2O_3 > 40				
Heavy mineral sandstone	TiO_2 > 8				
Dolerite	CaO > 10				
Silcrete + Siltstone	Limited sample				

these elements are less prone to matrix absorption or mineralogical effects (Wu et al., 2020). The raw material categories were determined based on the chemometry of the specimens. The elemental conditions that were used are presented in Table 2 and were determined based on: a. the p-XRF analyses on the micromorphology blocks, b. the macroscopic characteristics, c. petrographic literature.

4. Results

4.1. Macroscopic analysis

Sandstone rocks are characterized by the presence of distinct mineral grains of sand-sized particles that are cemented together (Fig. 4A-B, Fig. 5A-B). In some cases of coarse-grained sandstones, the grains were visible to the naked eye while in well-cemented pieces the use of the magnifying glass was necessary. Hornfels appeared homogeneous, dense, fine-grained without distinguishable minerals, a darker grey/green color, and often exhibiting semi-conchoidal fracture (Fig. 4C-D, Fig. 5C-D). 25 % of the hornfels deriving from spits 50 and 60 were noted to have a coarser texture (Fratta, 2022). Quartz was easily identified by its vitreous appearance, transparency or translucency, and its colorless to pale-white color (Fig. 4E). A way to macroscopically differentiate between hornfels and sandstone is to examine the specimens against a light source. The sandstone fragments are transparent at the edges due to the quartz grains.

4.2. Microscopic analysis

Through petrographic analysis of the UMH micromorphology thin sections, we recognized six lithologies: 1. sandstone, 2. hornfels, 3. quartz, 4. dolerite, 5. siltstone, and 6. silcrete.

1. The largest category is arenite sandstone (Folk, 1980) (Fig. 6A-B, Table 3). The arenite sandstone is poorly sorted with grain sizes ranging from ~ 50 to ~ 500 μm (Fig. 6A-B). The mineralogy is predominantly subrounded quartz grains (~95 %) that are bound by siliceous cement. Grains in the form of rock fragments (mostly chert) are also present while no feldspar grains were observed.

2. Hornfels is consistently present throughout the analyzed samples (Table 3). Overall, the hornfels pieces have planar-parallel fabrics, variation in color (greyish, yellowish-white, greenish, black, etc.), and often demonstrate a 'spotted' appearance (Fig. 6C-D). This spotted texture is common in contact metamorphic rocks and are the result of new minerals beginning to form (low pressure < 2kbar, medium to high temperatures 300–700 °C) (Mason, 1990). The mineral grains in the hornfels sections are not easily distinguishable as their forebear was

Table 3
Context of micromorphology samples, some of which yielded multiple studied thin-sections, and p-XRF samples, as well as, quantification of stone fragments based on micromorphology results. The stratigraphic location of the micromorphology samples is illustrated in Fig. 3, for the subdivision of units into spits refer to Table 1.

Context of samples					Micromorphological quantification of stone fragments										
Sample ID	Thin Section	Unit	Spit	N. p-XRF	Quartz		Sandstone		Hornfels		Silt. + Silcr.		Dolerite		N. Total
					N.	%	N.	%	N.	%	N.	%	N.	%	
UMH_12	12A	H10/P1			1	50			1	50					2
	12B						1	100							1
UMH_15	15	P2							1	100					1
UMH_13	13	P3	30	32	1	20	3	60	1	20					5
UMH_14	14	P5/P6/P8			10	56	5	28	3	17					18
UMH_5	5	P8			4	57	2	29	1	14					7
UMH_3	3A	P6/P7	50	74	1	33	1	33	1	33					3
	3B	P6/P7				0	5	25	12	60	3	15			20
UMH_6	6A	P10/P9				0	3	30	7	70					10
	6B	P10/P9				0	7	54	5	38					13
UMH_4	4A	P9	60	23	2	14	5	36	6	43			1	7	14
	4B	P9				0	13	87	1	7			1	7	15
UMH_35	35A	P14/P16	110	48	11	69	5	31							16
	35B	P14/P16			2	22	6	67	1	11					9
	35C	P14/P16			5	45	2	18	3	27			1	9	11
				Total	N		**37**		**58**		**43**			**3**	**3**	**145**
					%		**25.5**		**40.0**		**29.7**			**2.1**	**2.1**	**100**

Table 4
Summary of the representation of different raw materials in the piece-plotted assemblages from the spits examined in this analysis. We have piece-plotted all stone materials, also those that we consider natural pieces (natural sandstone fragments may derive from the shelter bedrock). Hence a separate column was added for natural and anthropogenic sandstone lithics. All other lithics are anthropogenic. Note that results from the visual identification and pXRF analysis differ for some pieces, refer to the supplementary information for details.

Spit		Sandstone				Quartz		Hornfels				Others		Total
		Anthrop.		Natural				Hornfels		Hornfels ↓K_2O ↑CaO				
		N	%	N	%	N	%	N	%	N	%	N	%	N
30	**Visual**	12	36	8	24	9	27	4	12	NA	NA	-[1]	–	33
	pXRF	11	33	8	24	9	27	4	12	NA	NA	1	3	33
50	**Visual**	15	20	3	4	2	3	54	73	NA	NA	1	1	74
	pXRF	15	20	3	4	2	3	52[2]	70	2	3	–	–	74
60	**Visual**	5[3]	22	1	4	2	9	3	13	11	48	1	4	23
	pXRF	6	26	1	4	2	9	7	30	4	17	3[4]	13	23
110	**Visual**	12	25	12	25	11	23	12	25	NA	NA	1	2	48
	pXRF	12	25	12	25	12[5]	25	11	23	NA	NA	1[6]	2	48
Total	**Visual**	44	25	24	13	24	13	73	41	11	6	3	2	178
	pXRF	44	25	24	13	25	14	74	42	6	3	5	3	178

[1] Piece visually determined as sandstone in pXRF analysis revised to ironstone.
[2] Piece on visual determination unknown revised to hornfels on pXRF analysis.
[3] Artefact visually classified as unknown revised to sandstone on pXRF analysis.
[4] Three pieces visually determined as coarse hornfels revised to unknown on pXRF analysis.
[5] Piece visually determined as unknown determined as quartz on pXRF.
[6] Piece visually determined as hornfels determined as unknown on pXRF.

most likely pyelitic (clay-rich) sediments. Lighter minerals are expected to correspond to quartz and feldspar while darker minerals present are biotite, andalusite, and pyroxene.

3. Quartz is observed roughly as frequently as hornfels (Table 3). The quartz from the uppermost samples (e.g., UMH_14, UMH_5) has distinct characteristics in comparison to the quartz from the lower sample (UMH_35). The main petrological difference is the presence of secondary granoblastic quartz within the lower samples (Fig. 6E-F). Additionally, the average size of the quartz fragments within the thin sections tends to increase in the lowermost deposits (~1 cm) compared to the upper Pleistocene deposits (~0.5 cm).

4. Dolerite (alias diabase) was observed in single instances in samples UMH_6, UMH_4, and UMH_35 (Table 3). It shows an interstitial texture between porphyritic and aphanitic mostly containing interlocking, lath-shaped plagioclase phenocrysts (Fig. 6G-H).

5. A total of two siltstone fragments was identified in the micromorphological thin sections (sample UMH_3, Table 3). They are characterized by interlocking silt-sized quartz crystals and iron-rich minerals (Fig. 6I-J, L).

6. One silcrete fragment was present in thin section UMH_3 (Table 3, Fig. 6I-K). It is characterized by cryptocrystalline and chalcedonic silica cement. Silcrete petrographic thin sections deriving from outcrops within the Pinnacle Point area (South Africa) were used as reference material (provided by Dr. Karkanas, Wiener Lab, ASCSA).

4.3. Portable X-ray fluorescence results

The complete raw data of the p-XRF measurements can be found in the Supplementary Material. Measurements conducted on the raw material categories on micromorphological blocks appear to be within the same range as those on the single stone finds (Fig. 7). Elemental values of sandstone and quartz show less variation, most probably due to their homogeneous composition (quartz-dominant) with quartz displaying lower concentrations for most elements (Fig. 7A-B, Supplementary Material). The compositional variation of hornfels is much higher compared with sandstone and quartz. We observe that hornfels pieces have higher Al_2O_3, K_2O, Fe_2O, Sr, Rb, and Ba concentrations emphasizing its pelitic origin (Fig. 7, Supplementary Material).

Fig. 4. View of specimens belonging to various raw material categories. A. Sandstone flake, specimen 3820; B. Heavy mineral sandstone roof spall, specimen 6698; C. Hornfels shaping flake, specimen 3758; D. Coarse hornfels elongated flake, specimen 4460; E. Quartz bipolar flake, specimen 4454; F. Ironstone fragment; specimen 1765 (Photos by Sofie Blik & Vi Fratta).

From the compositional variation plots of the hornfels pieces, two groups can be defined: a lower-K_2O and a higher- K_2O group. The lower-K_2O group demonstrates higher concentrations in CaO, Fe_2O_3, Cu and lower concentrations of K_2O, Rb, Th and Nb (Fig. 7). All the lower-K_2O pieces are distinguishable macroscopically due to their coarser texture (Fig. 4D). However, only 35% of the macroscopically coarser hornfels specimens were found to have a lower K_2O.

Some of the macroscopically-identified sandstone pieces demonstrated distinctive elemental compositions characterized by high concentrations of TiO_2, Cu, Nb, Zr, and Cr (see Supplementary Material). This sandstone sub-group was named heavy mineral sandstone. After re-examining the pieces, we did not distinguish any macroscopic difference from the other sandstone finds (Fig. 4A-B). After remeasuring, one of the 'heavy mineral sandstone' specimens (ID 6670) was identified as 'sandstone'. The other such finds were also remeasured and consistently yielded the high concentrations of TiO_2, Cu, Nb, Zr, and Cr.

One new raw material category, named ironstone, was identified based on outliers of the p-XRF results. The name of this category is descriptive since there has been no link to materials observed in the petrological thin sections, precluding assignment to a formal geological category. The ironstone has high values of Fe_2O_3, Sn, Th, V, and Pb (Supplementary Material). It is distinguishable macroscopically and was also recognized during the initial visual identification. Macroscopically, it appears as a sedimentary rock composed of fine-grained oxide phases like manganese and hematite which give a distinctive dark-red color (Fig. 4F).

4.4. Lithic analysis

Arenite sandstone is one of the most represented lithologies in the thin-sections and piece-plotted materials. As this also represents the shelter bedrock, we cannot use thin section data to determine whether

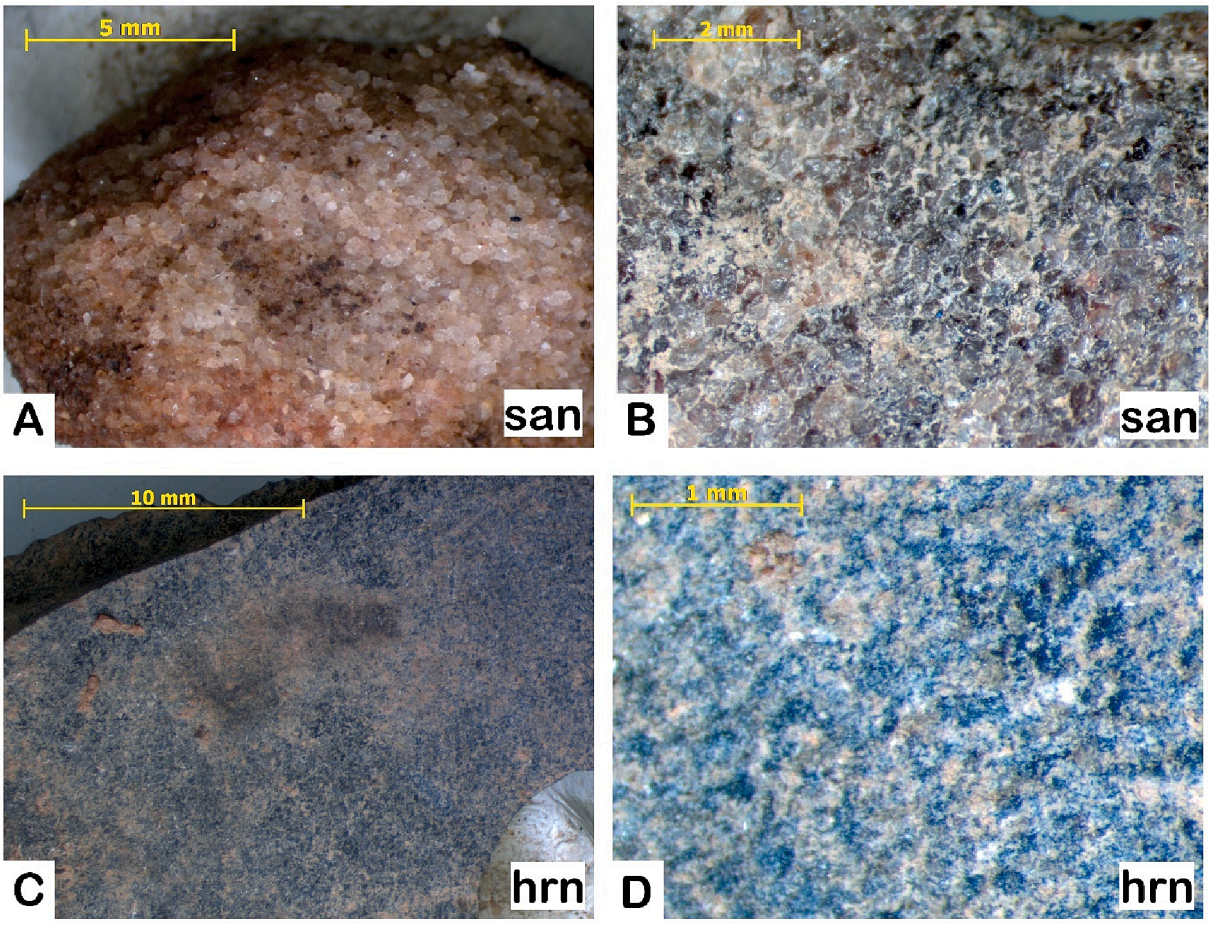

Fig. 5. Textural view from sandstone (san) (A, B) and hornfels (hrn) (C, D) specimens by stereomicroscope. A. Specimen 6746, Magnification 1.25x; B. Specimen 1726, Magnification 2.5x; C. Specimen 1761, Magnification 1x; D. Specimen 1761, Magnification 5x (Photos by B. van Os).

the sandstone pieces are anthropogenic or natural. Nevertheless, 65% of the piece-plotted specimens examined in this study have been determined as anthropogenic due to clear knapping stigmata, versus 35% natural roof spall (Supplementary Material; Table 4). All other raw material categories (hornfels, quartz, etc.) were transferred to the site by humans and all their observations in thin-sections and piece-plotted assemblages thus considered to be anthropogenic.

5. Discussion

5.1. Umhlatuzana raw materials

5.1.1. Raw material categories

By following a multi-method analytical protocol, this study reveals the use of raw materials of the UMH assemblage that were not previously identified, notably sandstone and one instance of silcrete. Sandstone, quartz, and hornfels are the most commonly represented lithologies (Table 3; Table 4), while dolerite, siltstone, silcrete, and ironstone are infrequently present or only in specific parts of the sequence. The p-XRF results indicate that we can differentiate between the rocks based on the signal of specific elements (e.g., CaO, K_2O, Fe_2O_3, Sr, Rb, Ba) (Table 2). This was also demonstrated by Wadley and Kempson (2011) on hornfels and dolerite from Sibhudu Cave. Consequently, we will continue to refine our protocol and make use of p-XRF in the ongoing lithic analysis to understand the variability of other raw material categories classified as 'Unknown' macroscopically.

The presence in the micromorphological thin-sections of rock types unreported in the piece-plotted sample may be explained by the fact that the analysed micromorphological samples represent a larger part of the stratigraphic sequence (Fig. 3). Nevertheless, as the analyzed thin sections only contain a very small part of lithics compared to the total, it stands to reason that not all rock types were found present. Indeed, p-XRF analysis of single finds ultimately revealed a new raw material category, ironstone, as well as subgroups within sandstone and hornfels (see section 4.2). Rock types high in Fe_2O_3, like the ironstone, were present in the thin sections but were assigned to 'ochre' and were not included in this study (also see 3.1). It is thus likely that the lithic finds identified as ironstone by p-XRF correspond to such 'ochre' pieces in the thin sections. The distinction of the two hornfels types, both macroscopically (Fratta, 2022) and based on their elemental signal (p-XRF) is something that will be further examined during the lithic analysis. Most likely the low-K_2O hornfels is derived from clay-rich metasediments that contained more carbonate. The high-K_2O group most likely contains more clay minerals, as is supported by its higher K_2O, Rb and Th contents (Fig. 7). When it comes to the heavy mineral sandstone pieces, the higher concentration of heavy minerals might represent sub-facies that still belong to the Ordovician Natal Group Formation. While most sandstone pieces are already attributed to the sandstone of the rockshelter bedrock, it is possible that the heavy mineral sandstone derives from a different sandstone outcrop.

5.1.2. Difference between 1980 s campaign and renewed excavations

Sandstone was a raw material category not identified in the previously published dataset (Kaplan, 1990). Sandstones and quartzites are very similar in terms of lithological and geomorphological characteristics and are thus frequently discussed in the same context (Auler, 2012). In this study, we limit the use of the term quartzite to rocks of a metamorphic origin. Some older sandstone classifications, including ones

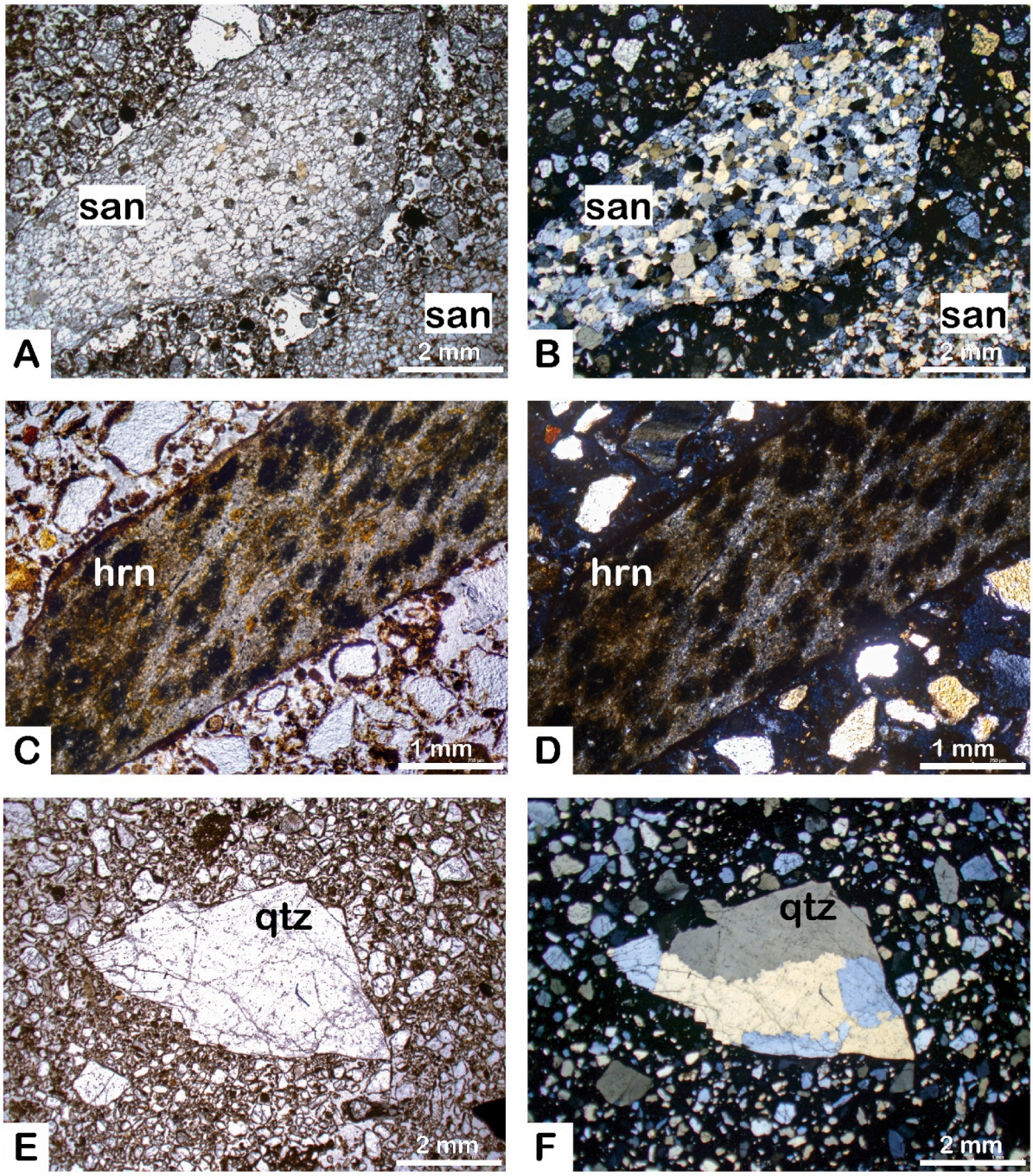

Fig. 6. Micrographs of the main raw material categories: A. Sandstone (san) (Thin section UMH_9B, PPL); B. Same as A in XPL; C. Hornfels (hrn). Note the spotted texture (Thin section UMH_9A, PPL); D. Same as C. in XPL; E. Quartz (qtz) (Thin section UMH_14, PPL); F. Same as E. in XPL. G. Dolerite (dol) (Thin section UMH_4B, PPL); H. Same as G. in XPL; I. Photomicrograph of silcrete (silc) and two siltstone (silt) fragments (Thin section UMH_3B, PPL); J. Same as I in XPL; K. Silcrete fragment in higher magnification (Thin section UMH_3B, PPL); L. Siltstone fragment in higher magnification (Thin section UMH_3B, XPL).

used in South Africa, categorized quartz arenites as quartzites (Adams, 1984; Howard, 2005). We note that Kaplan, and Lombard's subsequent studies, refer to UMH's bedrock as orthoquartzite, a term that is geologically equivalent to quartz arenite (Kaplan, 1990; Lombard et al., 2010). It is thus possible that what Kaplan identified as quartzite is what we identify as sandstone. In light of our piece-plotted sample and ongoing study, the previous analysis' estimate of the proportion of quartz still appears high (Schmid et al., forthcoming). One explanation could be that Kaplan's definition of quartz included different rock types, such as the sandstone. Another possibility is that most of the sandstone pieces were considered as natural objects deriving from the rockshelter itself and excluded from the raw material counts.

5.1.3. *Contextualization of results in southern Africa*

Accurate raw material characterization is essential in Stone Age archaeology as the data serve to understand technological and techno-economic choices of hunter gatherers. Subsequently the information allows to hypothesize about subsistence (e.g., Floss and Kieselbach, 2004; Morala and Turq, 1991; Moreau, 2009), land use as well as mobility of past societies and ultimately, to formulate models on

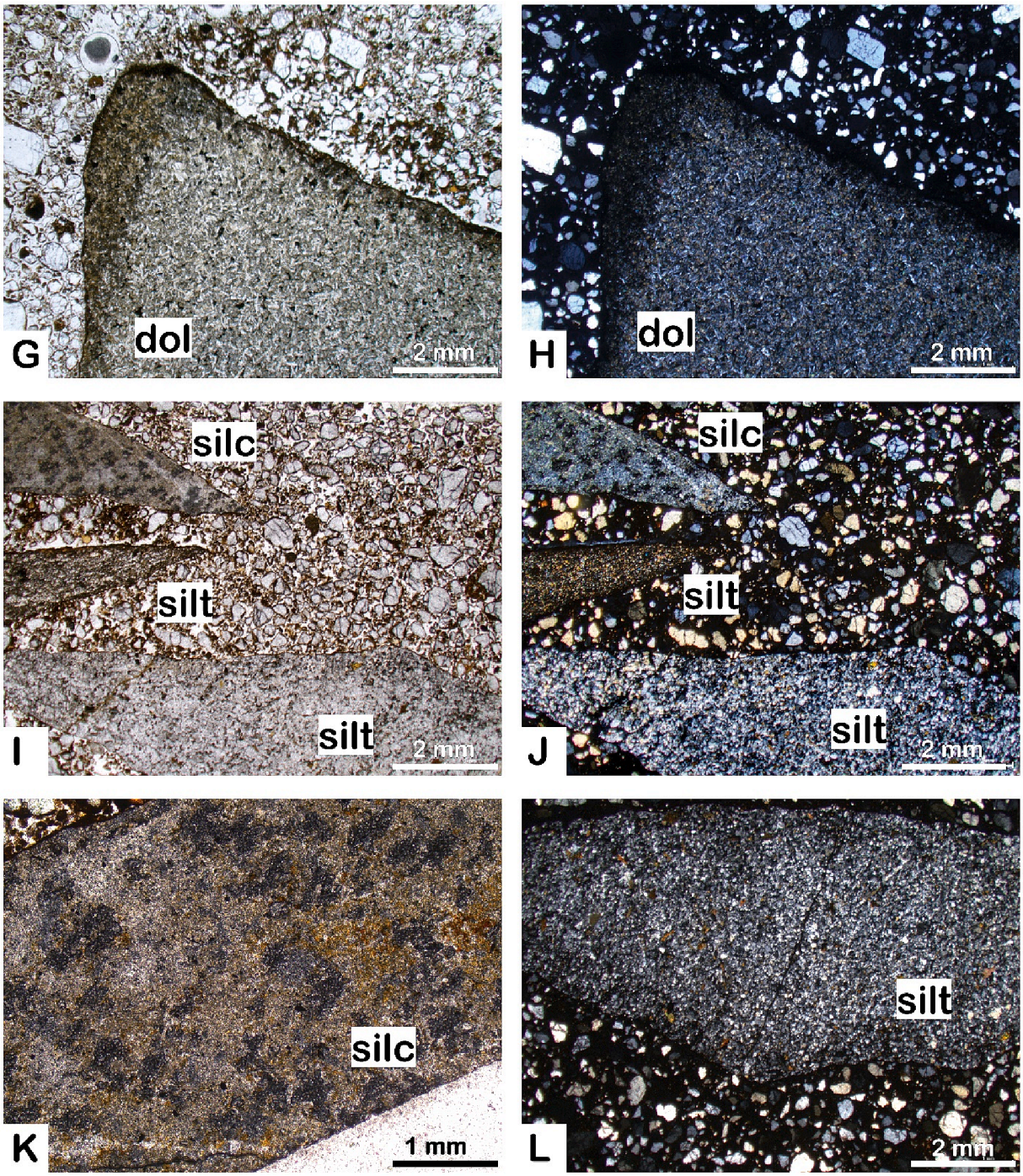

Fig. 6. (*continued*).

knowledge transfer, technological variability, and cultural change (e.g., Mackay et al., 2014; Stewart and Jones, 2016).

The clarification concerning the raw material composition of UMH changes our understanding of its raw material economy. The application to a small but representative sample documents the importance of an ultra-local raw material, namely the arenite sandstone that forms the bedrock. The relative proportions of quartz and hornfels also shift compared to previous results to a more equal representation of the two instead of a dominant use of quartz. Our ongoing lithic analysis will establish if this pattern can be applied to the sequence as a whole. With this increased comparability, we observe clearer correspondences in terms of raw material use with the cultural sequences of Sibhudu Cave and Umbeli Belli from the same region and of quasi-synchrony over periods of time (Bader et al., 2015, 2018, 2022; de la Peña, 2015; de la Peña and Wadley, 2017; Rots et al., 2017; Schmid et al., 2019; Villa et al., 2005; Wadley, 2005, 2013; Will and Conard, 2018). This is because Umhlatuzana shares similarities with the sequences at Sibhudu Cave and Umbeli Belli both typo-technologically and in terms of raw material provisioning and use, with the selection of sandstone attested at all of these sites (Bader et al., 2018; de la Peña and Wadley, 2017; Umbeli Belli ongoing micromorphology study). However, our study stresses that likewise at these two sites, the distinction and determination of quartzite and sandstone should be well-defined. Additional questions and exact percentages on the raw material variation in the sequence will be provided in our forthcoming publication in which we provide detailed technological description and raw material

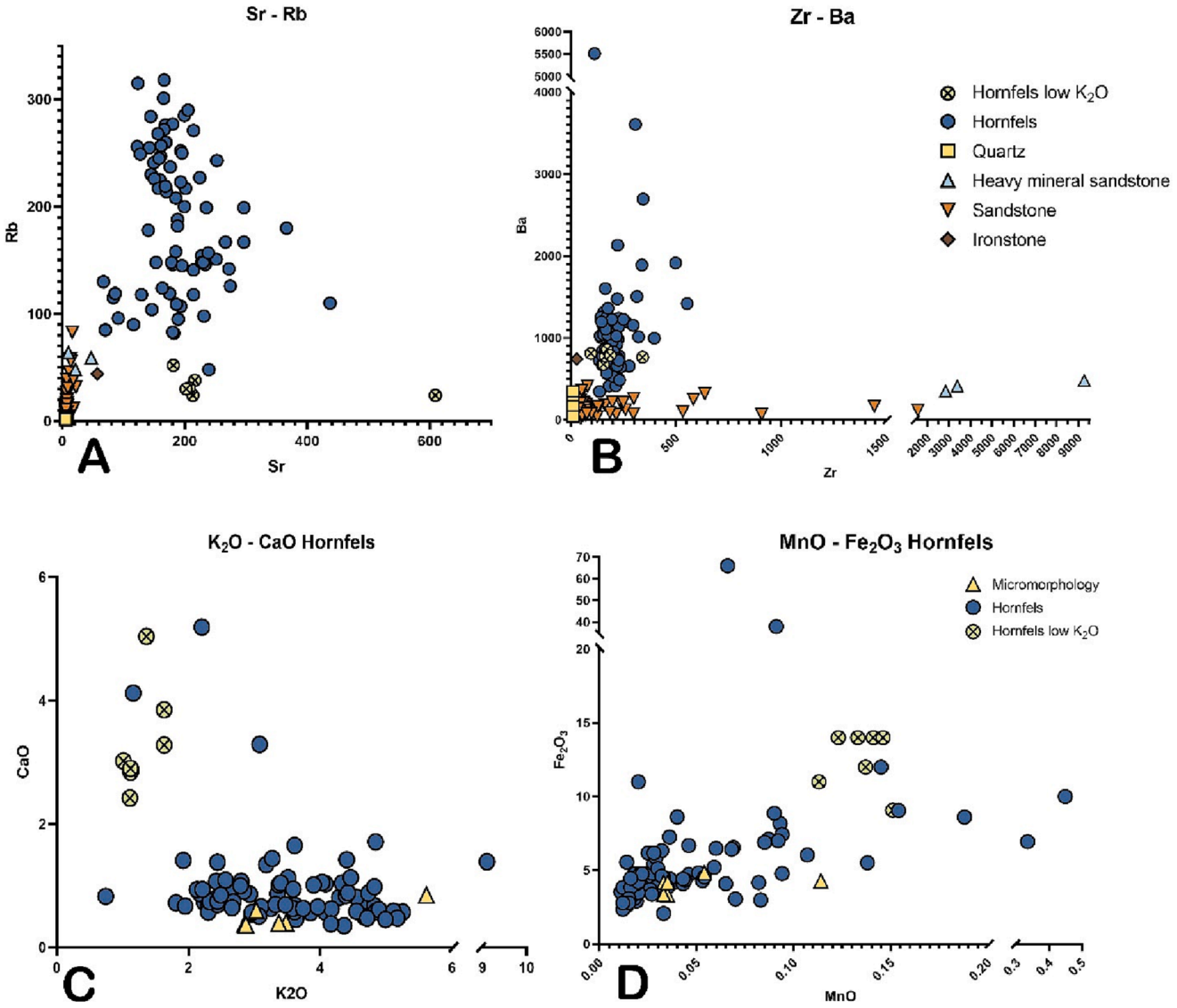

Fig. 7. P-xrf correlation plots for selected elements. a. sr-rb correlation plot of all the specimens; b. zr-ba correlation plot of all the specimens; c. k_2O-CaO plots on hornfels specimens; D. MnO-Fe_2O_3 plots on hornfels specimens.

identification of finds deriving from the renewed excavations (Schmid et al., forthcoming).

5.2. A raw material determination workflow

Macroscopic raw material identification methods provide qualitative data and are often preferred due to practical reasons such as high speed and low cost. While visual determinations can be effective (e.g., Doperalski, 2013), relying only on them often can lead to inconsistencies in classification and erroneous groupings of raw material categories (e.g., Boulanger et al., 2005; Milne et al., 2009; Rácz et al., 2016). Analytical techniques (e.g., petrography, geochemistry) provide complementary petro-archaeological data (e.g., Fernandes, 2012; Delvigne, 2016; Tomasso et al., 2019). However, these methods are more expensive and time consuming which makes them only feasible to apply to a selection of the assemblage or for specific research questions.

We propose that for accurate and efficient determinations of lithic raw material both visual and analytical methods should be applied (also see Milne et al., 2009). The first step would be to establish a raw material database, based on geological maps, literature review, and surveys, that is in agreement with the regional geology (Fig. 8). A macroscopic evaluation of the rock types is necessary (ideally by consulting a geologist), but it should be further supplemented by analytical techniques to confirm/adjust the initial assessment or to understand the variability of the raw materials. It is also crucial to bridge the quantitative characteristics of the analytical methods to the qualitative characteristics. The second step for the raw material identification consists solely of a visual categorization. In order to accomplish this, it is important to train the eye for an accurate identification based on the established database and/or have comparative pieces ready. An important third step would be to test the inter-observer consistency of the visual identification. This can be achieved by applying analytical techniques on a sub-sample and by following a visual evaluation protocol (e.g., Agam and Wilson, 2018). Finally, further analyses can be conducted on specimens that are not easily visually determined as well as outliers.

5.3. Protocol assessment

Following the raw material determination workflow has greatly improved the accuracy of macroscopic raw material identification. The initial raw material identification directly from the excavation and without cleaning was inaccurate in 13 % of the cases (Supplementary

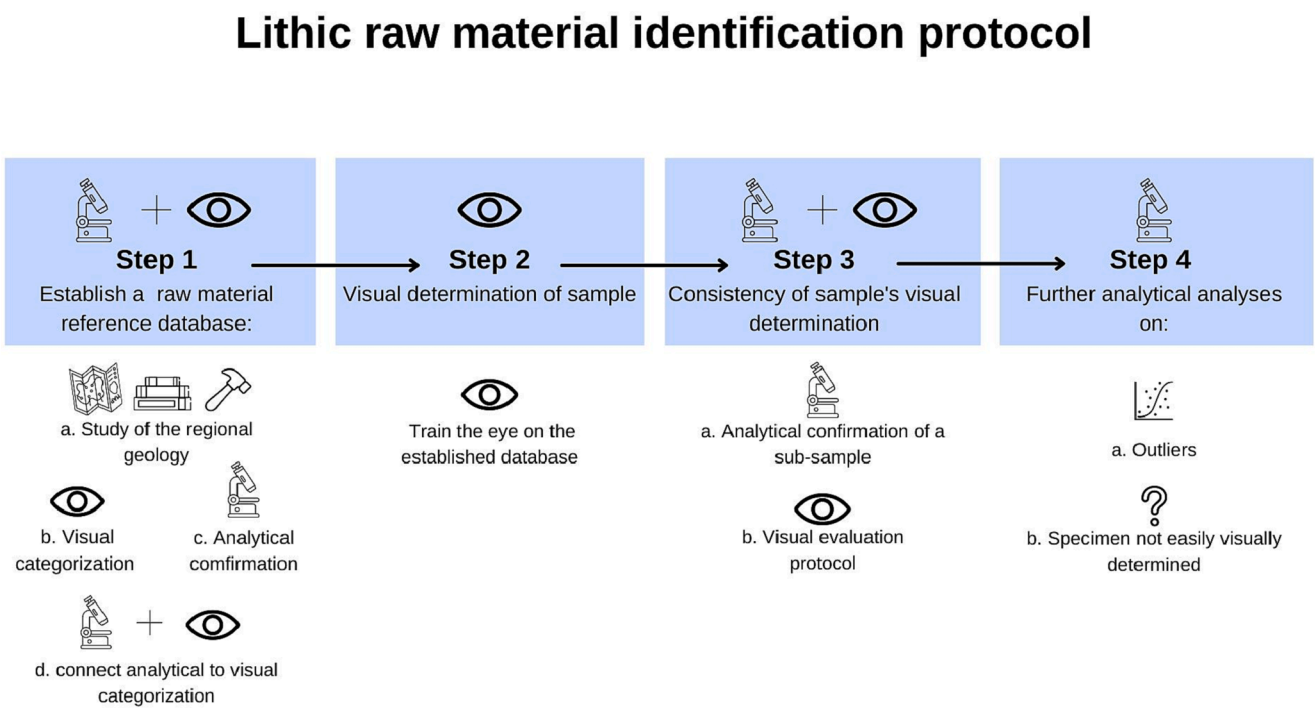

Fig. 8. Visualization of lithic raw material identification protocol using macroscopic and analytical raw material identification methods.

Material). After the finds were washed, a second macroscopic identification occurred in which 5 % of the finds were not accurately identified (Supplementary Material). In the ongoing technological analysis, the misidentification rate is much lower; this will be further discussed in the forthcoming publication concerning the UMH lithic assemblages.

Micromorphology and p-XRF are the two analytical techniques used in this study. Micromorphology provides informative insights not only into the category of materials encountered, but also their relative abundance across the sequence. Being able to grasp the petrological properties of a stone is crucial for an accurate determination of its rock type. In most of the cases, the micromorphological results are not truly integrated within the lithic technological studies. We demonstrate that micromorphological thin-section analysis provides complementary data to archaeological lithic analyses. The exact lithologies of archaeological materials are sometimes better studied through thin-sections. Here this led to the documentation of the presence of sandstone and the absence of previously reported quartzite. Other cases are presented by sites where rock types may be patinated or severely weathered, complicating raw material assessment. The differentiation between anthropogenic rocks and lithic artefacts cannot be performed on thin sections, here the complementary nature of traditional lithic analysis comes into its own. We therefore argue that where micromorphological analysis is conducted, the results should be integrated with lithic analysis at an early stage. Regarding the p-XRF analysis, we were able to use the results to accurately differentiate between the raw material categories. Our combined protocol establishes for a sample of assemblages throughout the Pleistocene sequence of Umhlatuzana the presence of anthropogenic sandstone artefacts structurally above 20 % of the total lithic sample.

6. Conclusion

This study provides preliminary insights into raw material selection during the Pleistocene occupational sequence of UMH. The results are used in the ongoing lithics analysis of the material excavated during the renewed excavations that will provide definite data on raw material variation through time. Moreover, this study prompted the creation of a raw material assessment workflow combining visual and analytical methods. This workflow ensures accurate and efficient determinations and can be applied to a wide spectrum of archaeological assemblages.

The combination of micromorphological and p-XRF analysis to investigate the lithic materials from UMH demonstrates that if only visual inspection is performed, the variability of raw materials used may be underestimated. The reliability of raw material determination is increased by applying geoarchaeological techniques. Ensuring that raw material categories are accurate, represents a necessary first step before reaching statements about raw material selection and furthermore, addressing techno-economic questions.

The protocol developed here brings increased resolution to studies of prehistoric raw material provisioning. The combination of petrographic observations and lithic determinations, with p-XRF measurements as secure data bridging the thin-section piece-plotted artefacts has increased insight into the proportions of different raw materials used and has highlighted previously unobserved varieties of raw materials at the site. With such applications, synthesizing analyses of economic or technological adaptations (e.g., Ambrose and Lorenz, 1990; Dusseldorp, 2014) and statistical approaches (e.g. McCall & Thomas 2009) can be performed on a more secure footing.

CRediT authorship contribution statement

Irini Sifogeorgaki: Conceptualization, Data curation, Formal analysis, Visualization, Methodology, Project administration, Supervision, Writing – original draft. **Viola C. Schmid:** Data curation, Formal analysis, Validation, Visualization, Writing – original draft. **Bertil van Os:** Data curation, Formal analysis, Resources, Software, Investigation, Methodology. **Vi Fratta:** Formal analysis, Investigation, Software, Visualization. **Hans Huisman:** Supervision, Validation. **Gerrit L. Dusseldorp:** Formal analysis, Funding acquisition, Investigation, Supervision, Validation, Writing – review & editing.

Declaration of Competing Interest

The authors declare that they have no known competing financial interests or personal relationships that could have appeared to influence

the work reported in this paper.

Data availability

Data will be made available on request.

Acknowledgements

We thank V. van den Brink, V. Madinani, F. Reidsma, J. Dekker, G. Halewijn, M. Pandolfi, S. Blik, C. Thornhill, A. Sokela, and L. van Schalkwyk for assistance in the field and processing of material. We are grateful to the KwaZulu-Natal Museum, Department of Human Sciences, G. Blundell, G. Laue, Phumulani Madonda, M. Munzhedzi, D. Tlhoalele, and G. Whitelaw who supported our excavations. We gratefully acknowledge AMAFA aKwaZulu-Natali, SAHRA, B. Pawandiwa, and S. Uys for issuing the requisite permits. We thank N. Skarpelis and P. Karkanas for their input in the raw material petrology. We are grateful to participants of the Rock and Roll: International symposium for knappable material 2021 conference for input on preliminary results of this study. We thank the SAS for providing a research support award to I. Sifogeorgaki visit the Wiener Lab in Athens. Finally, we want to thank the editing team and two reviewers for the helpful feedback on an earlier version of this paper. The research is funded by an NWO Vidi Grant 276-60-004 awarded to G. Dusseldorp.

Appendix A. Supplementary data

Supplementary data to this article can be found online at https://doi.org/10.1016/j.jasrep.2023.103890.

References

Adams, A.E., MacKenzie, W.S., Guilford, C., 1984. Atlas of sedimentary rocks under the microscope. Routledge, London.

Agam, A., Wilson, L., 2018. Blind test evaluation of consistency in macroscopic lithic raw material sorting. Geoarchaeology 34, 467–477. https://doi.org/10.1002/GEA.21720.

Ambrose, S.H., Lorenz, K.G., 1990. Social and eological models of the Middle Stone Age in southern Africa pp. In: Mellars, P. (Ed.), The Emergence of Modern Humans. Edinburgh University Press, Edinburgh, pp. 3–33.

Andrefsky, W., Andrefsky Jr, W., 1998. Lithics. Cambridge University Press, Cambridge.

Archer, W., Pop, C.M., Gunz, P., McPherron, S.P., 2016. What is Still Bay? Human biogeography and bifacial point variability. J. Hum. Evol. 97, 58–72. https://doi.org/10.1016/j.jhevol.2016.05.007.

Archer, W., Pop, C.M., Rezek, Z., Schlager, S., Lin, S.C., Weiss, M., Dogandžić, T., Desta, D., McPherron, S.P., 2018. A geometric morphometric relationship predicts stone flake shape and size variability. Archaeol. Anthropol. Sci. 10, 1991–2003.

Auler, A.S., 2012. Quartzite caves of South America. In: White, W., Culver, D. (Eds.), Encyclopedia of Caves. Academic Press, Amsterdam, pp. 850–860.

Bader, G.D., Will, M., Conard, N.J., 2015. The lithic technology of Holley Shelter, Kwazulu-Natal, and its place within the MSA of southern Africa. South African Archaeol. Bull. 70, 149–165.

Bader, G.D., Tribolo, C., Conard, N.J., 2018. A return to Umbeli Belli: New insights of recent excavations and implications for the final MSA of eastern South Africa. J. Archaeol. Sci. Reports 21, 733–757. https://doi.org/10.1016/j.jasrep.2018.08.043.

Bader, G.D., Schmid, V.C., Kandel, A.W., 2022. The Middle Stone Age of South Africa. Oxford Research Encyclopedia of Anthropology, Oxford.

Barker, A.J., 2014. A key for identification of rock-forming minerals in thin section. CRC Press/ Balkema, Leiden.

Barut, S., 1994. Middle and Later Stone Age lithic technology and land use in East African savannas. African Archaeol. Rev. 1994 121 12, 43–72. https://doi.org/10.1007/BF01953038.

Bertouille, H., 1989. Théories physiques et mathématiques de la taille des outils préhistoriques. FeniXX, Paris.

Bordes, F., 1947. Etude comparative des differentes techniques de taille du silex et des roches dures. Anthropologie 51, 1–29.

Boulanger, M., Hathaway, A., Speakman, R., Glascock, M., 2005. A Preliminary Study on the Suitability of Instrumental Neutron Activation Analysis (INAA) for Identifying Hathaway Formation Chert from the Northern Champlain Valley of Vermont. Archaeol. East. North Am. 33, 105–126.

Brandl, M., Martinez, M.M., Hauzenberger, C., Filzmoser, P., Nymoen, P., Mehler, N., 2018. A multi-technique analytical approach to sourcing Scandinavian flint: Provenance of ballast flint from the shipwreck "Leirvigen 1", Norway. PLoS One 13, e0200647.

Calvert, S.E., Pedersen, T.F., 2007. Elemental Proxies for Palaeoclimatic and Palaeoceanographic Variability in Marine Sediments: Interpretation and Application. In: Hilaire-Marcel, C., De Vernal, A. (Eds.), Developments in Marine Geology. Elsevier, pp. 567–644. https://doi.org/10.1016/S1572-5480(07)01019-6.

Clark, A.M.B., 1997. The MSA/LSA transition in southern Africa: new technological evidence from Rose cottage cave. South African Archaeol. Bull. 52, 113–121. https://doi.org/10.2307/3889076.

Cologne, D., Mourre, V., 2009. Quartzite et quartzites aspects pétrographiques, économiques et technologiques des matériaux majoritaires du Paléolithique ancien et moyen du Sud-Ouest de la France. In: Grimaldi, S., Cura, S. (Eds.), Etude Technologiques Sur L'exploitation Du Quartzite. Actes Du XV Congres Mondial de l'Union Internationale Des Sciences Prehistoriques et Protohistoriques. BAR International Series, pp. 3–12.

de la Peña, P., 2015. Refining our understanding of Howiesons Poort lithic technology: the evidence from Grey rocky layer in Sibudu cave (KwaZulu-Natal, South Africa). PLoS One 10, e0143451.

de la Peña, P., Wadley, L., 2017. Technological variability at Sibudu Cave: The end of Howiesons Poort and reduced mobility strategies after 62,000 years ago. PLoS One 12, e0185845.

Delvigne, V., 2016. Géoressources et expressions techno-culturelles dans le sud du Massif central au Paléolithique supérieur: des déterminismes et des choix. Bull. la Société Préhistorique Française 113, 613–615.

Delvigne, V., Fernandes, P., Bindon, P., Bracco, J.P., Klaric, L., Lafarge, A., Langlais, M., Piboule, M., Raynal, J.P., 2019. Geo-resources and techno cultural expressions in the south of the French Massif Central during the Upper Palaeolithic: determinism and choices. Anthropologica et Praehistorica, Bruxelles: Société Royale Belge d'Anthropologie et de Préhistoire 128, 39–55.

Dibble, H.L., Rezek, Z., 2009. Introducing a new experimental design for controlled studies of flake formation: results for exterior platform angle, platform depth, angle of blow, velocity, and force. J. Archaeol. Sci. 36, 1945–1954.

Doperalski, M.W., 2013. An Assessment of the Limitations of Macroscopic Lithic Raw Material Identification and Parent Nodule Assignment within Archaeological Contexts in Minnesota and an Analysis of Lithic Raw Material Utilization at 21LN2. University of Minnesota. MA Thesis.

Dusseldorp, G.L., 2014. Explaining the Howiesons Poort to post-Howiesons Poort transition: a review of demographic and foraging adaptation models. Azania: Archaeological Research in Africa 49, 317–353.

Favreau, J., Soto, M., Nair, R., Bushozi, P.M., Clarke, S., DeBuhr, C.L., Durkin, P.R., Hubbard, S.M., Inwood, J., Itambu, M., Larter, F., Lee, P., Marr, R.A., Mwambwiga, A., Patalano, R., Tucker, L., Mercader, J., 2020. Petrographic Characterization of Raw Material Sources at Oldupai Gorge, Tanzania. Front. in Earth Sci. 8, 158.

Fernandes, P., 2012. Itinéraires et transformations du silex: une pétroarchéologie refondée, application au Paléolithique moyen. Phd-thesis. Université de Bordeaux 1.

Floss, H., Kieselbach, P., 2004. The Danube Corridor after 29.000 BP: new results on raw material procurement patterns in the Gravettian of Southwestern Germany. Mitteilungen der Gesellschaft für Urgeschichte 13, 61–78.

Folk, R., 1980. Petrology of Sedimentary Rocks. Hemphill, Austin.

Fratta, V., 2022. Leaving No Stone Unturned: Raw Material Variability within the Umhlatuzana Rock Shelter Middle Stone Age in KwaZulu-Natal. Leiden University. BA Thesis.

Grove, M., Blinkhorn, J., 2020. Neural networks differentiate between Middle and Later Stone Age lithic assemblages in eastern Africa. PLoS One 15, e0237528. https://doi.org/10.1371/JOURNAL.PONE.0237528.

Högberg, A., Lombard, M., 2016a. Indications of pressure flaking more than 70 thousand years ago at Umhlatuzana Rock Shelter. South African Archaeol. Bull. 53–59.

Högberg, A., Lombard, M., 2016b. Still Bay point-production strategies at Hollow Rock Shelter and Umhlatuzana Rock Shelter and knowledge-transfer systems in southern Africa at about 80–70 thousand years ago. PLoS One 11, e0168012.

Howard, J., 2005. The Quartzite Problem Revisited. J. Geol. 113, 707–713. https://doi.org/10.1086/449328.

Huisman, D.J., van der Laan, J., Davies, G.R., van Os, B.J.H., Roymans, N., Fermin, B., Karwowski, M., 2017. Purple haze: Combined geochemical and Pb-Sr isotope constraints on colourants in Celtic glass. J. Archaeol. Sci. 81, 59–78. https://doi.org/10.1016/J.JAS.2017.03.008.

Kaplan, J.M., 1989. 45000 Years of Hunter-Gatherer History in Natal as Seen from Umhlatuzana Rock Shelter. Goodwin Ser. 6, 7–16. https://doi.org/10.2307/3858128.

Kaplan, J., 1990. The Umhlatuzana Rock shelter sequence: 100 000 years of Stone Age history. Natal Museum J. Humanit. 2, 1–94.

Kieffer, G., Raynal, J.-P., 2007. Pétroarchéologie des roches volcaniques, in: Raynal J.-P., (Ed.), Sainte-Anne I, Sinzelles Polignac. Haute-Loire: Le Paléolithique Moyen de l'unité J. Laussonne, 47–58.

Lombard, M., 2007. The gripping nature of ochre: the association of ochre with Howiesons Poort adhesives and Later Stone Age mastics from South Africa. J. Hum. Evol. 53, 406–419.

Lombard, M., Wadley, L., Jacobs, Z., Mohapi, M., Roberts, R.G., 2010. Still Bay and serrated points from Umhlatuzana Rock Shelter, Kwazulu-Natal, South Africa. J. Archaeol. Sci. 37, 1773–1784. https://doi.org/10.1016/J.JAS.2010.02.015.

Mackay, A., Stewart, B.A., Chase, B.M., 2014. Coalescence and fragmentation in the late Pleistocene archaeology of southernmost Africa. J. Hum. Evol. 72, 26–51.

MacKenzie, W., Adams, A., 1994. A color atlas of rocks and minerals in thin section. Manson Publishing, London.

Mason, R., 1990. Petrology of the metamorphic rocks, 2nd ed. Springer, Netherlands.

McCall, G.S., Thomas, J.T., 2009. Re-examining the South African Middle-to-Later Stone Age transition: Multivariate analysis of the Umhlatuzana and Rose Cottage Cave

stone tool assemblages. Azania Archaeol. Res. Africa 44, 311–330. https://doi.org/10.1080/00672700903337519.
Milne, B.S., Hamilton, A., Fayek, M., 2009. Combining visual and geochemical analyses to source chert on Southern Baffin Island, Arctic Canada. Geoarchaeology 24, 429–449. https://doi.org/10.1002/GEA.20273.
Mohapi, M., 2008. A new angle on Middle Stone Age hunting technology in South Africa, University of the Witwatersrand. Azania Archaeol. Res. Africa 44, 161–162.
Mohapi, M., 2013. The Middle Stone Age point assemblage from Umhlatuzana rock shelter: A morphometric study. South. African Humanit. 25, 25–51.
Morala, A., Turq, A., 1991. Relations entre matières premières lithiques et technologie: l'exemple du Paléolithique entre Dordogne et Lot. In: 25 ans d'études technologiques et préhistoriques: bilan et perspectives. Actes des XIe Rencontres Internationales d'Archéologie et d'Histoire d'Antibes, 18–20 octobre 1990, Juan-le-Pins, 159-168.
Moreau, L., 2009. Geißenklösterle – Das Gravettien der Schwäbischen Alb im europäischen Kontext. Kerns Verlag, Tübingen.
Mourre, V., 1996. Les industries en quartz au Paléolithique. Terminologie, méthodologie et technologie. Paléo. Rev. d'Archéologie Préhistorique 8, 205–223.
Pargeter, J., 2016. Lithic miniaturization in Late Pleistocene southern Africa. J. Archaeol. Sci. Reports 10, 221–236. https://doi.org/10.1016/J.JASREP.2016.09.019.
Pelegrin, J., 2000. Les techniques de débitage laminaire au Tardiglaciaire: critères de diagnose et quelques réflexions, in: Bodu, P., Valentin, P., Christensen, M., (Eds.), L'Europe Centrale et Septentrionale au Tardiglaciaire; Confrontation des modèles régionaux, Nemours, pp. 73–86.
Porraz, G., Igreja, M., Schmidt, P., Parkington, J.E., 2016. A shape to the microlothic Robberg from Elands Bay Cave (South Africa). South African Humanit. 29, 203–247.
Potts, P.J., Webb, P.C., 1992. X-ray fluorescence spectrometry. J. Geochem. Explor., Geoanal. 44, 251–296. https://doi.org/10.1016/0375-6742(92)90052-A.
Prieto, A., Ysta, I., Arrizabalaga, A., 2020. From petrographic analysis to stereomicroscopic characterisation: a geoarchaeological approach to identify quartzite artefacts in the Cantabrian Region. Archaeol. and Anthrop. Sci. 12, 1–23.
Rácz, B., Szakmány, G., Biró, K.T., 2016. Contribution to the cognizance of raw materials and raw material regions of the transcarpathian palaeolithic. Acta Archaeol. Acad. Sci. Hungaricae 67, 209–229. https://doi.org/10.1556/072.2016.67.2.1.
Reidsma, F.H., Sifogeorgaki, I., Dinckal, A., Huisman, H., Sier, M.J., van Os, B., Dusseldorp, G.L., 2021. Making the Invisible Stratigraphy Visible: A Grid-Based, Multi-Proxy Geoarchaeological Study of Umhlatuzana Rockshelter South Africa. Front. Earth Sci. 9, 520. https://doi.org/10.3389/FEART.2021.664105/BIBTEX.
Rots, V., Lentfer, C., Schmid, V.C., Porraz, G., Conard, N.J., 2017. Pressure flaking to serrate bifacial points for the hunt during the MIS5 at Sibudu Cave (South Africa). PLoS One 12, e0175151.
Saini-Eidukat, B., Michlovic, M.G., 2005. Material Analysis of Lithic Flaking Debris. Plains Anthropol. 50, 159–167.
Sánchez de la Torre, M., Utrilla, P., Domingo, R., Jiménez, L., Bourdonnec, F.-X., Gratuze, B., 2020. Lithic raw material procurement at the Chaves cave (Huesca, Spain): A geochemical approach to defining Palaeolithic human mobility. Geoarchaeology 35, 856–870. https://doi.org/10.1002/GEA.21808.
Šarić, K., Šarić, J.A., Cvetković, V., 2021. Advanced petrographic study of chipped stone artefacts from Lepenski Vir (Serbia): Evidence for across-Danube communication in the Mesolithic? Quat. Sci. Rev. 252, 106741.
Schmid, V.C., Porraz, G., Zeidi, M., Conard, N.J., 2019. Blade Technology Characterizing the MIS 5 DA Layers of Sibudu Cave South Africa. Lithic Technol. 44, 199–236.
Schmid, V.C., Sifogeorgaki, I., Abbruzese, T., Blik, S., Huang, L., Dusseldorp, G.L. forthcoming. A snapshot on Middle to Later Stone Age technological developments from Umhlatuzana Rock Shelter.
Shipton, C., Roberts, P., Archer, W., Armitage, S.J., Bita, C., Blinkhorn, J., Courtney-Mustaphi, C., Crowther, A., Curtis, R., Errico, F. d', Douka, K., Faulkner, P., Groucutt, H.S., Helm, R., Herries, A.I.R., Jembe, S., Kourampas, N., Lee-Thorp, J., Marchant, R., Mercader, J., Marti, A.P., Prendergast, M.E., Rowson, B., Tengeza, A., Tibesasa, R., White, T.S., Petraglia, M.D., Boivin, N., 2018. 78,000-year-old record of Middle and Later Stone Age innovation in an East African tropical forest. Nat. Commun. 2018 91 9, 1–8. https://doi.org/10.1038/s41467-018-04057-3.
Sifogeorgaki, I., Klinkenberg, V., Esteban, I., Murungi, M., Carr, A.S., van den Brink, V.B., Dusseldorp, G.L., 2020. New Excavations at Umhlatuzana Rockshelter, KwaZulu-Natal, South Africa: a Stratigraphic and Taphonomic Evaluation. African Archaeol. Rev. 37, 551–578. https://doi.org/10.1007/s10437-020-09410-w.
Skarpelis, N., Carter, T., Contreras, D.A., Mihailović, D.D., 2017. Characterization of the siliceous rocks at Stélida, an early prehistoric lithic quarry (Northwest Naxos, Greece), by petrography and geochemistry: A first step towards chert sourcing. J. Archaeol. Sci. Reports 12, 819–833. https://doi.org/10.1016/J.JASREP.2016.11.015.
Soressi, M., Geneste, J.-M., 2011. The history and efficacy of the *Chaîne Opératoire* approach to lithic analysis: Studying techniques to reveal past societies in an evolutionary perspective. PaleoAnthropology 334–350.
Steele, T., Mackay, A., Fitzsimmons, K., Marwick, B., Orton, J., Schwortz, S., Stahlschmidt, M., Igreja, M., 2016. Varsche Rivier 003: A Middle and Later Stone Age Site with Still Bay and Howiesons Poort Assemblages in Southern Namaqualand, South Africa. PaleoAnthropology 2016, 100–163. https://doi.org/10.4207/PA.2016.ART101.
Stewart, B.A., Jones, S.C., 2016. Africa from MIS 6–2: the florescence of modern humans. In: Jones, S., Stewart, B. (Eds.), Africa from MIS 6-2. Springer, pp. 1–20.
Stoops, G., 2003. Guidelines for analysis and description of soil and regolith thin sections. Soil Science Society of America, Madison, Wis.
Stoops, G., Nicosia, C., 2017. Sampling for Soil Micromorphology. Archaeological Soil and Sediment Micromorphology. In: Nicosia, C., Stoops, G. (Eds.), Archaeological Soil and Sediment Micromorphology. Wiley, pp. 383–391. https://doi.org/10.1002/9781118941065.ch35.
Theys, J., Webb, J., Cosgrove, R., 2019. Sourcing hornfels artefacts in eastern Tasmania: Understanding Aboriginal mobility in a lithic-rich landscape. J. Archaeol. Sci. Reports 26, 101883. https://doi.org/10.1016/j.jasrep.2019.101883.
Tomasso, A., Binder, D., Fernandes, P., Milot, J., Léa, V., 2019. The Urgonian chert from Provence (France): the intra-formation variability and its exploitation in petro-archeological investigations. Archaeol. Anthropol. Sci. 11, 253–269.
Tryon, C.A., Faith, J.T., 2016. A demographic perspective on the Middle to Later Stone Age transition from Nasera rockshelter, Tanzania. Philos. Trans. R. Soc. B Biol. Sci. 371, 20150238. https://doi.org/10.1098/RSTB.2015.0238.
Villa, P., Delagnes, A., Wadley, L., 2005. A late Middle Stone Age artifact assemblage from Sibudu (KwaZulu-Natal): comparisons with the European Middle Paleolithic. J. Archaeol. Sci. 32, 399–422.
Wadley, L., 2005. A typological study of the final Middle Stone Age stone tools from Sibudu Cave, KwaZulu-Natal. South African Archaeol. Bull. 60, 51–63.
Wadley, L., 2013. MIS 4 and MIS 3 Occupations in Sibudu, KwaZulu-Natal, South Africa. South African Archaeol. Bull. 68, 41–51.
Wadley, L., Kempson, H., 2011. A review of rock studies for archaeologists, and an analysis of dolerite and hornfels from the Sibudu area, KwaZulu-Natal. South. Afr. Humanit. 23, 87–107.
Will, M., 2021. The Role of Different Raw Materials in Lithic Technology and Settlement Patterns During the Middle Stone Age of Southern Africa. African Archaeol. Rev. 38, 477–500.
Will, M., Conard, N.J., 2018. Assemblage variability and bifacial points in the lowermost Sibudan layers at Sibudu, South Africa. Archaeol. Anthropol. Sci. 10, 389–414.
Wu, L., Wilson, D.J., Wang, R., Yin, X., Chen, Z., Xiao, W., Huang, M., 2020. Evaluating Zr/Rb Ratio from XRF Scanning as an Indicator of Grain-Size Variations of Glaciomarine Sediments in the Southern Ocean. Geochem., Geophys., Geosyst. 21, e2020GC009350. https://doi.org/10.1029/2020GC009350.